



Phosphorus recovery as struvite from hydrothermal carbonization liquor of chemically produced dairy sludge by extraction and precipitation

Claver Numviyimana^{a,*}, Jolanta Warchol^a, Nidal Khalaf^b, James J Leahy^b, Katarzyna Chojnacka^a

^a Department of Advanced Material Technology, Faculty of Chemistry, Wrocław University of Science and Technology, ul. M. Smoluchowskiego 25, Wrocław 50-372, Poland

^b Department of Chemical Sciences & Engineering, University of Limerick, Limerick V94 T9PX, Ireland

ARTICLE INFO

Editor: Teik Thye Lim

Keywords:

Phosphorus recovery
Struvite precipitation
Phosphorus extraction
Iron recycling
Dairy sludge

ABSTRACT

Phosphorus (P) recovery from dairy wastewater involves its accumulation into phosphorus-rich sludge using a physico-chemical or biological process. The high iron content in chemical sludge decreases its usability in agricultural activities. The hydrothermal carbonization (HTC) is an option used to treat the sludge to obtain hydrochar for various applications, including its use as an energy source and as a carbon-dense material. The HTC process leaves a bigger volume of nutrient-rich liquor, which phosphorus (P) purification was the subject of this work. By direct precipitation, the product iron content was 17.96%, a value higher than accepted limits for phosphate fertilizers. Thus, P extraction followed by struvite precipitation was studied. The use of oxalic acid extracted 86.7% of P from HTC liquor, while 86.6% of iron was removed. The process conditions of pH 9, and salt dosage of 1.73:1.14:1 for Mg:NH₄⁺:P mole ratio for struvite precipitation were obtained with a P recovery of 99.96%, and the effluent P concentration below 2 mg·L⁻¹. The quality of products as fertilizers was tested by both in-vitro and in-vivo assays. High iron content in the product demonstrated a negative effect on plant germination, whilst the precipitation product from P extract demonstrated an advantage of P purification into struvite for plant macro and micronutrient availability. The used method of P extraction followed by struvite precipitation is useful for both P and iron recovery into two separate products with agricultural and chemical applications, respectively.

Nomenclature

AE	Agronomic efficiency
ANR	Apparent nutrient recovery
DM	Dry matter
DOE	Design of experiments
EDS	Energy dispersive spectroscopy
HTC	Hydrothermal carbonization
L-HTC	Leachate of hydrothermal carbonization liquor
NER	Nutrient efficiency ratio
PE	Physiologic Efficiency
Q _e	Equilibrium sorption capacity
SEM	Scanning electron microscopy
SI	Saturation index

1. Introduction

Phosphorus (P) loss in the environment causes soil nutrient depletion which induces a decrease in crop production [1]. It roots into waterbody eutrophication due to an excess of phosphates from sewage and industrial effluents [2]. Dairy processing industries are among the largest food wastewater sources, especially in Europe [3]. The European Union (EU) currently leads the world milk production with annual records of approximately 160 million tonnes, which processing contributes to wastewater generation [4]. The P recovery from wastewater involves physicochemical process, biological process, and their combination [5]. In either case, the aim is to remove P from wastewater and accumulate it into a P-rich sludge [6]. The physicochemical processes are widely applied in wastewater treatment by involving, for example, the use of precipitating agents such as lime, alum, and iron salts; the combination of salts dosing with filtration techniques [7], and electrochemical

* Corresponding author.

E-mail address: claver.numviyimana@pwr.edu.pl (C. Numviyimana).

precipitation [8]. The chemical process demonstrates high P removal efficiency with adverse effect of enormous sludge generation [9]. This is due to high amount of metal salts added to decrease P concentration to the needed lower level in treated water. Iron salts dose as coagulants can vary from 1 to 2 mol ratio to P in order to have the P concentration less than $0.2 \text{ mg}\cdot\text{L}^{-1}$ in treated water [10]. For the purpose of shrinking the P concentration to less than $0.05 \text{ mg}\cdot\text{L}^{-1}$, the iron dose can be risen to 4 mol ratio to P [11]. Research highlighted many challenges caused by wastewater sludge, including their excessive production, the needs for disposal, and limitations of their application in agriculture [12,13]. Different strategies of sludge management have been subjects of studies including their incineration [14], their use in anaerobic co-digestion for energy recovery [15], and their use as substrate in production of biochar [16]. The amount of 8.7 million tonnes of sludge were produced in EU-member states in 2020, of which 47.7% was used in agriculture as fertilizer [14]. The challenging facts of direct agricultural use of sewage sludge include the environmental risk posed by micro-pollutants and pathogens [17]. The reported organic pollutants in sludge with various concentration range include poly-aromatic hydrocarbon (PAHs) which concentration ranged from 0 to $31 \text{ mg}\cdot\text{kg}^{-1}$, polychlorinated biphenyls (PCBs) with range of $0\text{--}3 \text{ mg}\cdot\text{kg}^{-1}$, and various concentrations of dioxins, and pharmaceuticals [18]. The micro-organisms are present in sludge with different range of concentration including viruses ($87\text{--}417 \times 10^7 \text{ cfu}\cdot\text{g}^{-1}$), bacteria ($2.69\text{--}3376 \times 10^5 \text{ cfu}\cdot\text{g}^{-1}$), helminths ($0.063\text{--}453.5 \text{ eggs}\cdot\text{g}^{-1}$), fungi ($114.3\text{--}752.3 \times 10^6 \text{ cfu}\cdot\text{ml}^{-1}$), and protozoa ($12\text{--}32 \text{ oocyst}\cdot\text{g}^{-1}$) [19]. In addition to those limitations, the efficiency of sludge as fertilizer is unstable because of low nutrient content, low nutrient release and variable nutrient composition [20]. Previous works highlighted that the supply of sludge as a fertilizer with high iron content decreased P availability for some crops [21]. The P availability to plant for iron based sludge was found to decrease with Fe: P molar ratio, where it was effectively plant-available up to a Fe: P mole ratio of 1.6, and decreased with higher mole ratios [22]. Such Fe:P mole ratio is easy to exceed in iron based sludge. Ashekuzzaman et al. (2019) has found that iron and P contents in a chemically produced dairy sludge with ferric salts were 162 and $31.6 \text{ g}\cdot\text{kg}^{-1}$, respectively, equivalent to 2.8 of Fe:P mole ratio [23]. The EU fertilizers regulation 2019/1009 does not include the sludge as fertilizing product on EU market. The limitation does not apply to valuable products obtained by sludge processing designated as STRUBIAS (struvite, biochar, ash) [24]. Therefore, searching for alternative options for valorization of iron based sludge and their transformation into more valuable products is important.

One of the options for organic waste treatment involves thermochemical processes such as hydrothermal carbonization (HTC). In that process, the organic wastes are heated with water in closed systems and produce a solid fraction (hydrochar) and a liquid fraction (liquor) [25]. The HTC valorizes wet organic wastes into solid hydrochar with better chemical, physical, and fuel properties compared with the raw biomass [26]. Despite that the aqueous phase can exceed 75% of substrate [27], the nutrients recovery from the produced liquor has known limited studies. The dissolved P in the liquor can be purified by precipitation into struvite, calcium phosphate or iron phosphate salts [28]. Struvite precipitation presents an advantage for its usability as a fertilizer, with the provision of P and nitrogen in an efficiently available form for plant nutrition [29]. The aim of this work was to recover P as struvite from the liquor of hydro-thermally processed P rich dairy sludge. This scenario presents advantages that hydrochar has various applications, including its use as a source of energy, contaminant removal such as heavy metals, carbon dioxide sequestration and its use as STRUBIAS material [30,31]. The HTC products are completely sterilized avoiding the presence of pathogenic organisms such as bacteria and viruses [32]. However, the high iron content in the liquor obtained from the HTC of iron-based sludge affects the quality of the precipitation product. Along with calcium, iron exhibits high precipitation potential and inhibitory properties of struvite [33,34]. This follows the lower water solubility (K_{sp}) for calcium phosphate salts such as hydroxyapatite ($\text{Ca}_5(\text{PO}_4)_3\text{OH}$, $K_{sp} = 2.1$

$\cdot 10^{-58}$) [33], and iron salt such as vivianite ($\text{Fe}_3(\text{PO}_4)_2\cdot 8\text{H}_2\text{O}$, $K_{sp} = 10^{-35.8}$) [35], than struvite ($\text{MgNH}_4\text{PO}_4\cdot 6\text{H}_2\text{O}$, $K_{sp} = 10^{-13.17}$) [36]. The product thereby formed contains an excess of iron and limits its application as fertilizer [37].

The European Commission regulation 2019/1009 sets a non-declarable maximum of 2% of non-chelated iron in inorganic solid fertilizers [38]. Thus, it is mandatory to apply methods which products meet market standards. This work undertook a feasibility study of P recovery as struvite from HTC liquor through extraction and precipitation processes. Previous works demonstrated the possibility of an extraction method for removal of heavy metal ions from leachate liquor by precipitation as sulphides [39]. On the other hand, oxalic acid demonstrated the settling property for iron [40]. The additional benefits of oxalic acid leachate are found in struvite reaction enhancement by decreasing calcium ion concentration, thus lowering the level of struvite inhibitors. Nevertheless, the oxalic acid extraction is not effective at removing trivalent ferric ions where they form soluble iron (III) oxalate that passes into the aqueous phase [41]. Thanks to the HTC process, in which in an acidic environment, the iron (III) is reduced efficiently by organic matter to Fe (II) removable as oxalate precipitate during the extraction process [42,43].

This experimental work aimed at the determination of process conditions for P purification from HTC liquor of dairy sludge through extraction and struvite precipitation. Furthermore, for the process nexus life cycle, natural zeolite property was assessed for residual ammonium removal to meet the low value of ammonium in the production effluent. Microscopic and spectroscopic analyses were used for product morphology and phase characterization, respectively. To highlight the relevance of the study, the nutrient availability to plants for organic waste and purified products was compared through experimental studies.

2. Material and methods

2.1. Sample and HTC treatment

Dairy sludge was collected from Arrabawn Company near Limerick (Ireland) and stored in a refrigerator at $4 \text{ }^\circ\text{C}$ in the laboratories of the University of Limerick (UL). The hydrothermal carbonization was performed using the 7.5 L PARR 4545 reactor. The sludge water content was 86% and a solution of 1% H_2SO_4 was added to reach a pH of 2.2 as initial conditions. The reaction temperature was controlled and the time needed by the heater to reach the set reaction temperature was 3 h. At that point, the stirrer was initiated at 25 rpm, and the temperature and pressure were monitored throughout the residence time. After 2 h, the reaction was terminated, and the reactor was left to cool down at ambient temperature, whereas the gases were released into the fume hood. In further steps, after cooling, the products were retrieved and the solid hydrochar was separated from the liquid portion through filtration. The solid fraction was dried in the oven at $105 \text{ }^\circ\text{C}$ for 24 h and was subject of study as STRUBIAS material for agricultural application, the work previously published by Shi et al. [31]. The liquor produced from the HTC was the subject of this work for P recovery as struvite. Both sludge and HTC liquor samples were characterized for the total concentration of elements using USEPA method 3051 and multi-elemental analysis by ICP-OES (ICP-OES Vista MPX, Varian) [44]. The total nitrogen and carbon were analyzed using the macro combustion Analyzer (Vario Macro Cube Elementary Analyzer GmbH, Langensfeld, Germany). The ammonium nitrogen was analyzed using a DR1900 portable spectrophotometer following the EPA method 350.1.

2.2. Phosphorus speciation in the liquor

The struvite and other salts of prompt recovery from the liquor were assessed based on saturation indices (SI) and solubility as per other works [34,45]. The change of a component activity follows the mass

balance equation. In fact, the amount of a component in a system remains constant regardless the undergone transformations [46]. Thus, the component conservation model (Eq. 1) is observed for P species in the solution.

$$TOT_j = C_j + \sum_i^N v_{ij}C_i \quad (1)$$

Where TOT_j is the total molal concentration of a component (j) involved in reactions; C_j , the actual concentration in solution; and the sum of N molal concentrations (C_i) of j binding species with v , the stoichiometric coefficient that equals the number of moles of j present in one mole of i^{th} species. For thermodynamic dependence, the concentration was corrected to activity (a_i), which equals to the molar concentration C_i multiplied by the activity coefficient (γ_i). The Eq. 1 for a component leads to a stoichiometric matrix of formed species and their components. The speciation takes into account the system's electro-neutrality, acid-base equilibria, and ionic strength [47]. For the accountability of all physical chemical interactions, the visual Minteq (version 3.1, KTH, Sweden) served in P speciation, ion activity product (IAP) and SI of sparingly soluble compounds [48].

2.3. Phosphorus extraction

To decrease the level of iron in the liquor sample, oxalic acid was studied for P extraction and iron removal from HTC liquor using a mimic solution [40]. Different concentrations (0.03, 0.061, 0.125, 0.1875, 0.25, and 0.375 mol·L⁻¹) of oxalic acid were evaluated. For the experiments where the pH failed to reach pH < 2 by the addition of extracting acid, the hydrochloric acid 5 M was added drop wise until the pH < 2. In fact, oxalic acid is a diprotic acid with two different acidity constants (pKa₁ = 1.27 and pKa₂ = 4.66) [49]. Below pH 2, this compound is in molecular and mono-protic ionic form, with the ability to form less soluble salts of iron (II) and calcium (II) oxalates. As the pH increases, the ionic form of the acid becomes more predominant and decreases its removal by chelating the metal ions in the supernatant. In addition to iron removal, the use of oxalic acid as an extracting solution removes calcium to a high extent. Despite the enhanced advantage of struvite crystallization, calcium is an important plant macronutrient and is worth keeping in the struvite product. Therefore, sodium sulphide was assessed for selective iron removal using a similar range of concentrations. The artificial solution mimicking HTC liquor was prepared in a 150 ml borosilicate glass beaker together with Na₂S concentration under a fume hood. Four milliliters of 5 M HCl solution were added per 100 ml sample volume to keep the pH less 2.5. The pH adjustment was to favor the dissolution of P and to avoid the precipitation of acidic calcium phosphate probable in the pH range from 4 to 6 [50]. The mixture was capped with parafilm paper and shaken at 20 rpm for 30 min, and settled for 2 h for separation. The supernatant was filtered using Wattman filter papers followed by elemental analysis.

2.4. Struvite precipitation

2.4.1. Instrumentation

The precipitation experiments were conducted in batch reactors equipped with a 1 L beaker, a water bath (PLWC 35 S, made in Poland), and a stirrer (CAT-100, made in Germany), at 22 °C, stirring speed of 60 rpm, for 1 h [51]. The pH adjustment was done by the addition of NaOH 6 M and monitored using a multifunction meter (CX-705 Elemen-tron). In addition to elemental analysis, the final products were characterized using X-ray diffraction (XRD) spectroscopy. The analysis consisted for 2θ from 10° to 50° with 0.01° steps and 0.50 speeds using the Rigaku MiniFlex diffractometer (Rigaku MiniFlex diffractometer, Tokyo, Japan) with copper anticathode ($\lambda = 1.54 \text{ \AA}$) following standard method EN-13925. The scanning electron microscopy (SEM/Xe-PFIB Microscope FEI Helios, with EDS detector) served in product

morphology and elemental mapping using standard method ISO 22309:2011. The product particle size analysis was conducted with a laser diffraction particle size analyzer (LS I3 320, BECKMAN COULTER) equipped with a dry powder sample system, sonication control unit, and personal computer.

2.4.2. Salt dosage and process conditions

The experimental investigation of process conditions and salt dosage was done on the P extract. The three level design of experiments (DOE) was done as previously [52] on artificial solutions considering three factors of pH, Mg: P, and NH₄⁺: P mole ratios with experimental ranges of 7.5–10.5, 1–2, and 0.2–1.2, respectively. The same procedures were applied to the sample without extraction to assess the effect of extraction on the quality of the precipitation product. In this case, the factor of foreign ions, mainly calcium and iron, were minimized to a 0.25 Ca: P mole ratio by additional P sources. In all runs, magnesium chloride 2 mol·L⁻¹, dipotassium hydrogen phosphate 1 mol·L⁻¹, and ammonium chloride 4 mol·L⁻¹ were used for Mg, P, and NH₄⁺ dosage, respectively. Besides the control doses of struvite precursors, a similar amount of iron chloride tetra-hydrate and calcium chloride di-hydrate as their metal molar content in the HTC liquor were part of the artificial sample. Experiments were conducted on a 2.5-fold dilute sample. The NaHCO₃ 0.25 M was added up to 10% for alkalinity adjustment and the mixture was upgraded to 1000 ml after pH adjustment. The evaluated outputs included efficiency of P removal (Rec P), struvite fraction in the product (X-NH₄⁺), and the efficiency of ammonium use in the reactor (RecN). The ammonium recovery from struvite precipitation effluent was assessed by a sorption process using natural zeolite [53]. In this case, natural clinoptilolite tuff was used. This zeolitic material was obtained from a mineral deposit located in the Nižný Hrabovec, Slovakia. The material consists of 74% clinoptilolite, 11% cristobalite, 6% plagioclase, 4% illite and smectite, 3% tridymite, 1% kaolinite and 1% quartz. The conditional equilibrium sorption capacity (Q_e) obtained after 5 h contact time with the effluents of all experimental runs was part of multiple optimization [54]. This was performed using a desirability function where modeled experimental yields were maximized, errors minimized while keeping all factors in range, except pH, which was maintained at 9 as found previously [55]. Further experiments were conducted to assess the effect of residence time for phase equilibrium and initial sample dilution factor (DF) on product particle size. The contribution to production cost effectiveness was calculated as per Bashar et al. [56] based on the used chemicals in P extraction, and struvite precipitation. The cost of magnesium salts and alkali were taken from previous work [56], while that of technical grade oxalic acid was estimated based on market price of the Universal Chemicals & Industries Pvt. Ltd (Indiamart, India).

2.5. Fertilizer product evaluation

2.5.1. In-vitro assay

The nutrient release kinetic study was conducted in citrate solution (Citric acid/KOH) at pH 6 and assessed the nutrient bioavailability through their in-vitro release assay (Eq. 2) [57,58].

$$C = C_{max}(1 - e^{-kt}) \quad (2)$$

With C_{max} , the maximum concentration of nutrients released in citric solution, and C , the dissolved nutrient concentration at time t , and k , the nutrient release rate constant. The C_{max} enables finding the bioavailability as a ratio of C_{max} to the initial nutrient amount in aliquot weight. Other parameters, such as the time t_{80} required to reach 80% of C_{max} , and time constant parameters (τ) were determined as per previous work [52]. The assay conducted on both raw organic wastes and their struvite products enabled the comparative study of the impact of P purification on nutrient availability.

2.5.2. In-vivo assay

A germination test was conducted on cucumbers (*Cornichon de Paris*) using a non-fertilized humic soil (Type TORF OGRODNICZY, Biotiva) with a high content of organic matter. The soil and struvite dose was suggested in other work [59]. In this experiment, 0.2 g of struvite product was used per 35 g of soil in which one seed was placed. The illumination was controlled by a specific lamp (Lamp LED Secret Jardin COSMORROW 20 W-Ultraviolet) and the plant watering was done daily after 24 h. The germinated seeds were counted after one week and the germination rate was calculated as a percentage of germinated seeds on the placed seeds. The nutrient use efficiency parameters were studied as per Baligar et al. [60]. These include nutrient efficiency ratio (NER) defined as the mass units' ratio of total plant yield to nutrient content; physiological efficiency (PE) defined as the yield mass on nutrient uptake for a fertilized trial after subtraction of control results; agronomic efficiency (AE) defined as the additional amount of economic yield, i.e., yield minus control per unit nutrient applied (m_f), and apparent nutrient recovery efficiency (ANR) used to reflect plant ability to acquire applied nutrients from soil [60]. Those aforementioned nutrient use efficiencies are calculated using Eqs. (3–6).

$$NER = \frac{Y}{C_i} \quad (3)$$

$$PE = \frac{Y_F - Y_C}{C_{i,F} - C_{i,C}} \quad (4)$$

$$AE = \frac{Y_F - Y_C}{m_f} \quad (5)$$

$$ANR = \frac{C_F - C_C}{m_f} \times 100 \quad (6)$$

With Y, the yield in kg; C_i , the mass content in kg of nutrient in biomass tissues; Y_F , Y_C , the yield in kg for fertilized and control trials, respectively; $C_{i,F}$, and $C_{i,C}$ are the nutrient uptake in kg for fertilized and control trials, respectively; m_f , amount of nutrient applied.

3. Results and discussion

3.1. Sample characteristics

The chemical composition of the sludge and the HTC liquor with their elemental molar ratios to P in the liquor is presented in Table 1. Considering the concentration of P in the liquor and their sludge, multivalent metal ions were immobilized in hydrochar and their small fraction were dissolved in the liquid phase. Such partition occurs due to the spontaneous binding of these metals with orthophosphate in the solution to form less soluble salts. For calcium, iron, and P, the dissolution rates were 11.25%, 7.02%, and 7.9%, respectively. This indicates

Table 1
Results of chemical analysis of dairy sludge (DS) and its HTC liquor (L).

Elements	Concentration (mg·kg ⁻¹)		Molar ratio to P for sample L	Elements	Concentration (mg·kg ⁻¹)		molar ratio to P for sample L
	DS	L			DS	L	
pH		6.96		N [%]	5.15	1.05	5.15
C [%]	48.70	3.72	<0.01	Na	3039.20	557.70	0.17
Al	6116.00	421	0.11	Ni	6.96	< LOD	–
B	1.65.00	2.52	<0.01	P	57,177	4517.00	1.00
Ba	16.00	0.55	<0.01	Pb	4.26	0.07	<0.01
Ca	49,205.00	5538.00	0.95	S	4321.40	1302.00	0.28
Co	0.10	0.74	<0.01	Sb	9.96	1.35	<0.01
Fe	12,8741.00	9033.00	1.11	Si	62.30	53.40	0.01
K	15,256.00	2382.00	0.42	Ti	580.20	1.64	<0.01
Mg	2874.70	278.60	0.08	V	5.53	0.38	<0.01
Mn	181.69	19.21	<0.01	Zn	125.80	15.20	<0.01
				NH ₄ ⁺		5850.00	2.87

their accumulation in hydrochar following the supersaturation of their phosphate salts.

The observed elemental partition matches up with the previous research, which found that iron and calcium phosphate were formed in hydrochar following their high content in HTC feedstock [25]. Despite the low dissolution rate, the concentration of P in HTC liquor was still high and made it a nutrient rich aqueous mixture for the recovery through precipitation process. The phosphorus species in the liquor estimated as per Eq. 1 are presented in Table 2. The results indicate that FeHPO₄ and FeH₂PO₄⁺ are the predominant phosphate species in the liquor, with 45% and 15% molar fraction of total phosphorus, respectively. Their preeminence is enhanced by high iron concentration and the pH conditions, where at the pH of the liquor, the H₂PO₄⁻ and HPO₄²⁻ species are the predominant forms of phosphate.

Considering the SI values of phosphate salts estimated at pH 9, the results show high SI for calcium and iron phosphate salts due to their high precipitation potential and the high concentration of P in the sample (Table 1). The salts of prompt recovery at pH 9 are presented in Table 3 with their SI. The iron precipitates as vivianite (SI = 19.6), while struvite lattice ions are in low concentration in the liquor and their precipitation is at a trace level (Section 3.5). According to Table 3, ammonium precipitates only as struvite and its fraction (X-NH₄⁺) in the formed product was used to assess the struvite precipitation efficiency. In this regard, further steps studied process conditions of iron removal by P extraction and proper dosage of struvite precursor salts.

3.2. Phosphorus extraction and Iron removal efficiencies

The extraction using oxalic acid indicated the effect of solvent concentration on removal efficiency (RE). The use of 0.375 mol·L⁻¹ solution of oxalic acid decreased iron concentration from 9033 to 1209 mg·L⁻¹ (i.e. up to 86.6% RE); whereas calcium concentration decreased from 5538 to 342 mg·L⁻¹ (i.e. up to 93.82% RE). In contrast, the phosphorus level did not change significantly. The latter decreased only by 13.4%. This P decrease in the extract can be due to sorption by calcium and iron oxalates precipitates [61]. On the other hand, the use of sodium sulphide was not effective for iron removal. At the same concentration of extracting agent of 0.375 mol·L⁻¹, the iron RE was only 23%. The main reason is the formation and evolution of hydrogen sulphide gas by hydrolysis of sodium sulphide. This phenomenon is caused by pH adjustment to a lower level (< 2.5) to favor P dissolution and to inhibit its precipitation into dicalcium phosphate salts. As pH is lowered by the addition of strong acid, the formed weak and volatile sulphide acid evolves and causes a decrease in iron (II) sulphide precipitation. In addition, the use of sodium sulphide as an extraction solution requires careful handling with sophisticated installation due to the generation of odors by its hydrolysis (S²⁻ + H₂O ↔ H₂S + OH⁻). The results for concentrations of extracting solutions in the range of 0.03–0.375 mol·L⁻¹ and the variation of iron and calcium RE are shown

Table 2
Stoichiometric speciation of phosphorus in the liquor.

Species	Components								Fraction %
	PO ₄ ³⁻	H ⁺	Zn ²⁺	Al ³⁺	K ⁺	Mg ²⁺	Ca ²⁺	Fe ²⁺	
HPO ₄ ²⁻	1	1							9.50
H ₂ PO ₄ ⁻	1	2							14.31
FeH ₂ PO ₄ ⁺	1	2						1	15.46
FeHPO ₄ (aq)	1	1						1	45.05
MgHPO ₄ (aq)	1	1				1			1.13
CaHPO ₄ (aq)	1	1					1		8.44
CaPO ₄ ⁻	1						1		0.30
CaH ₂ PO ₄ ⁺	1	2					1		1.14
KHPO ₄ ⁻	1	1			1				2.96
AlHPO ₄ ⁺	1	1		1					0.69
ZnHPO ₄ (aq)	1	1	1						0.02
K ₂ HPO ₄ (aq)	1	1			2				0.17
KH ₂ PO ₄ (aq)	1	2			1				0.85

Table 3
Stoichiometric matrix of possible phosphate salts in HTC liquor and their SI.

Possible salts	Components										HTC liquor	
	Al ³⁺	PO ₄ ³⁻	NH ₄ ⁺	Mg ²⁺	Ca ²⁺	Zn ²⁺	K ⁺	Fe ²⁺	H ⁺	H ₂ O	log IAP	SI
Ca ₃ (PO ₄) ₂		2			3						-19.64	9.28
Ca ₄ H(PO ₄) ₃ ·3H ₂ O(s)		3			4				1	3	-37.15	10.80
CaHPO ₄ (s)		1			1				1		-17.41	1.87
CaHPO ₄ ·2H ₂ O(s)		1			1				1	2	-17.47	1.53
Hydroxyapatite		3			5				-1	1	-21.91	22.42
K-struvite		1		1			1			6	-10.36	0.64
Mg ₃ (PO ₄) ₂ (s)		2		3						3	-21.90	1.38
MgHPO ₄ ·3H ₂ O(s)		1		1					1	3	-18.25	-0.08
Struvite		1	1	1						6	-9.84	3.42
Variscite	1	1								2	-20.61	1.46
Vivianite		2						3		8	-18.13	19.63

in Fig. 1.

Therefore, the struvite inhibition was mitigated through extraction using oxalic acid as the extracting solution. The oxalic acid 0.375 mol·L⁻¹ was used in further experiments.

3.3. Precipitation and related DOE results

Upon immediate precipitation at pH 9 without additional salt, the obtained product has a high content of calcium, iron, and phosphorus. This is due to the precipitation of amorphous calcium phosphate and vivianite. During this process, the P removal was up to 97.50% and 99.96% by experiments done with real and artificial solutions, respectively. Such removal efficiency highlights the ability of phosphate to form less soluble salts with a number of di- and tri-valent metals (see products *a* and *a'* in Table 4). In fact, the high iron level in the obtained product is restricted to the European market for phosphate fertilizer. The aim of extraction and DOE application was to extract phosphate, decrease iron and find the proper salt dosage to mitigate the negative effect of liquor composition on product quality. Up to 15 experiments were conducted for each mimic solution of the sample and the extract. Under this experimental investigation, the pH, magnesium, and nitrogen dosage demonstrated their significant effects ($p < 0.05$) on RecP, X-NH₄⁺, RecN, and Q_e. The experimental relationships were fitted with a determination coefficient better than 95%, good adequate precision (> 4), and a non-significant lack of fit. All factors were optimized with desirability D = 0.951. The pH was fixed at 9, the obtained optimum salt dosage was 1.73:1.14:1 as initial Mg: NH₄⁺: PO₄³⁻ mole ratio. The P recovery from the leachate was RecP = 99.96 ± 0.46%. The ammonium sorption from the effluent was Q_e = 1.25 mg NH₄⁺ per g of zeolite. The predicted and experimental X-NH₄⁺ were 6.76% and 7.28%, respectively. These conditions were applied to the HTC liquor after P extraction, and the product ammonium content was 6.69 ± 0.01%. Thus, the

struvite in the formed P product is estimated at 91.02%. The P and Fe concentration in the precipitation effluent was 1.7 and 1.09 mg·L⁻¹, respectively. Such concentration levels comply with the threshold limit of a maximum of 2 and 5 mg·L⁻¹ of P and iron in industrial effluent, respectively [62,63]. The ammonium in the effluent was 95.82 mg·L⁻¹, equivalent to 82.6% of its recovery from the feed sample. The ammonium concentration was decreased to less than 60 mg·L⁻¹ by addition of clinoptilolite (Q_e = 1.25 mg·g⁻¹) to fall into the accepted range with regard to EU decision 2018/1147 [64]. Additional DOE results are presented in Appendix A.

Considering the used sample, 52.5 kg of fertilizer can be produced from 1 m³ of HTC liquor. For the cost effectiveness, the used chemical dose contributes 1.80 €·kg⁻¹ and 12.62 €·kg⁻¹ to struvite production and P recovery costs, respectively. Additionally, the iron and calcium oxalates were recovered. This cost is affordable view the value of produced struvite enriched with proper content of iron, a plant essential micronutrient. Nevertheless, it alerts on possible high production and recovery cost at the full scale with accountability of operational and maintenance cost. The high production cost was previously reported per 1 kg P in range from 11 USD to 55 USD (i.e. nearly 9.52–47.61 €) while their products market prices ranges from 0.95 to 4 USD per 1 kg (i.e. nearly 0.82–3.46 €) [65].

3.4. Effect of dilution and residence time

The growth of phosphate precipitate was time and dilution (DF) dependent. After 1 h of precipitation reaction, the evaluated residence time for equilibrium indicated the increase in particle size with the residence time.

In the investigated process conditions, Fig. 2a shows that the high particle agglomeration is nearly 200 μm of particle diameter. The increase in residence time to 24 h indicates the agglomerated particle size

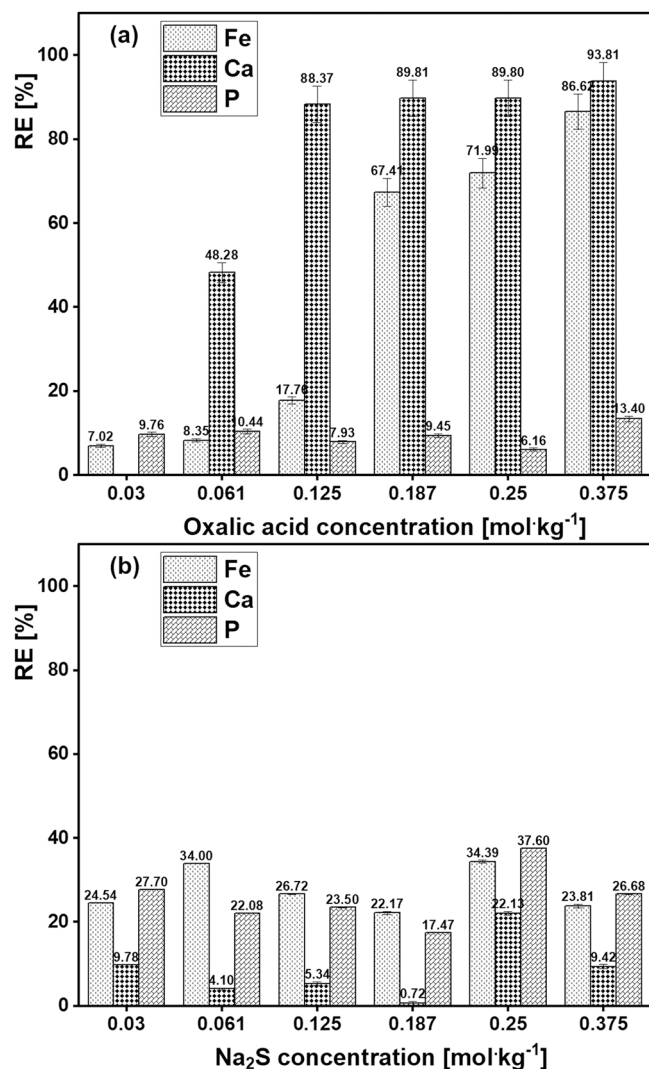


Fig. 1. Removal efficiency (RE) of iron and calcium during P extraction with oxalic acid (a) and sodium sulfide (b).

up to 600 μm . Additionally, the high initial concentration enhances the precipitate growth. The high particles' agglomeration was found when the sample was not diluted (DF1). Under these conditions, there is a visible increase in percentage volume with particle size to nearly 1000 μm (Fig. 2a). Considering the residence time, the particle size increased with equilibrium time. Nonetheless, the effluent P was stabilized to less than $2 \text{ mg}\cdot\text{L}^{-1}$ in supernatant up to 1 h equilibrium time (see Fig. 2b). This indicates that the crystal growth is more affected by initial concentration.

Table 4

Elemental characteristics of products obtained under different conditions.

ID [%]	Ca	Fe	K	Mg	P ₂ O ₅	NH ₄ ⁺	Na	Tot. C
a	8.04 ± 0.09	17.91 ± 0.01	0.33 ± 0.00	0.74 ± 0.04	28.20 ± 0.00	0.43 ± 0.01	1.23 ± 0.01	0.49 ± 0.000
a'	9.68 ± 0.02	17.42 ± 0.03	1.05 ± 0.00	0.44 ± 0.00	22.57 ± 0.00	2.33 ± 0.01	5.63 ± 0.01	0.61 ± 0.00
b	3.43 ± 0.03	6.65 ± 0.01	1.26 ± 0.00	6.23 ± 0.02	31.60 ± 0.07	6.49 ± 0.01	1.06 ± 0.01	4.83 ± 0.02
b'	5.21 ± 0.08	6.16 ± 0.01	0.84 ± 0.01	8.43 ± 0.03	25.05 ± 0.14	6.06 ± 0.00	1.56 ± 0.01	0.17 ± 0.00
c	1.99 ± 0.01	1.88 ± 0.00	0.53 ± 0.00	9.93 ± 0.01	28.18 ± 0.00	6.69 ± 0.01	5.64 ± 0.00	5.21 ± 0.04
c'	1.19 ± 0.00	1.11 ± 0.00	0.55 ± 0.01	11.17 ± 0.04	31.44 ± 0.00	7.28 ± 0.01	0.77 ± 0.00	0.18 ± 0.00
d	7.33 ± 0.05	11.04 ± 0.00	0.21 ± 0.00	1.53 ± 0.01	0.34 ± 0.00	1.72 ± 0.02	0.61 ± 0.00	18.71 ± 0.21
d'	11.94 ± 0.04	16.02 ± 0.05	0.65 ± 0.00	0.19 ± 0.00	3.68 ± 0.00	1.53 ± 0.01	0.18 ± 0.00	18.17 ± 0.33

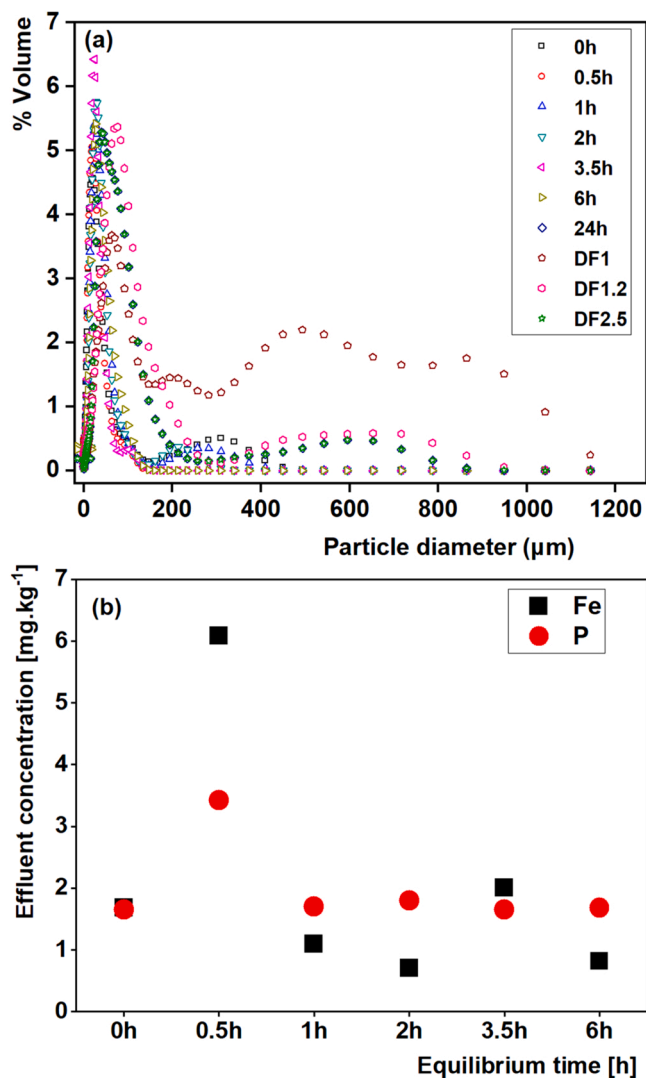


Fig. 2. Particle size variation with residence time and dilution factor (a), and effect of equilibrium time on P effluent concentration (b).

3.5. Characterization of recovered products

The products of direct salt recovery from the HTC liquor are highly iron and calcium-based phosphate products. This was observed for both real (a) and mimic (a') samples in Table 4. The optimized salts dosage without P extraction by additional ammonium, magnesium, and phosphorus sources to the HTC liquor enhanced struvite content (b and b' in Table 4). The product nitrogen content was improved, and the iron decreased from 17.42% to 6.16%. Despite the applied additional dose of struvite precursors, the obtained product does not meet the regulations of the phosphate fertilizer market with regard to iron content. This was

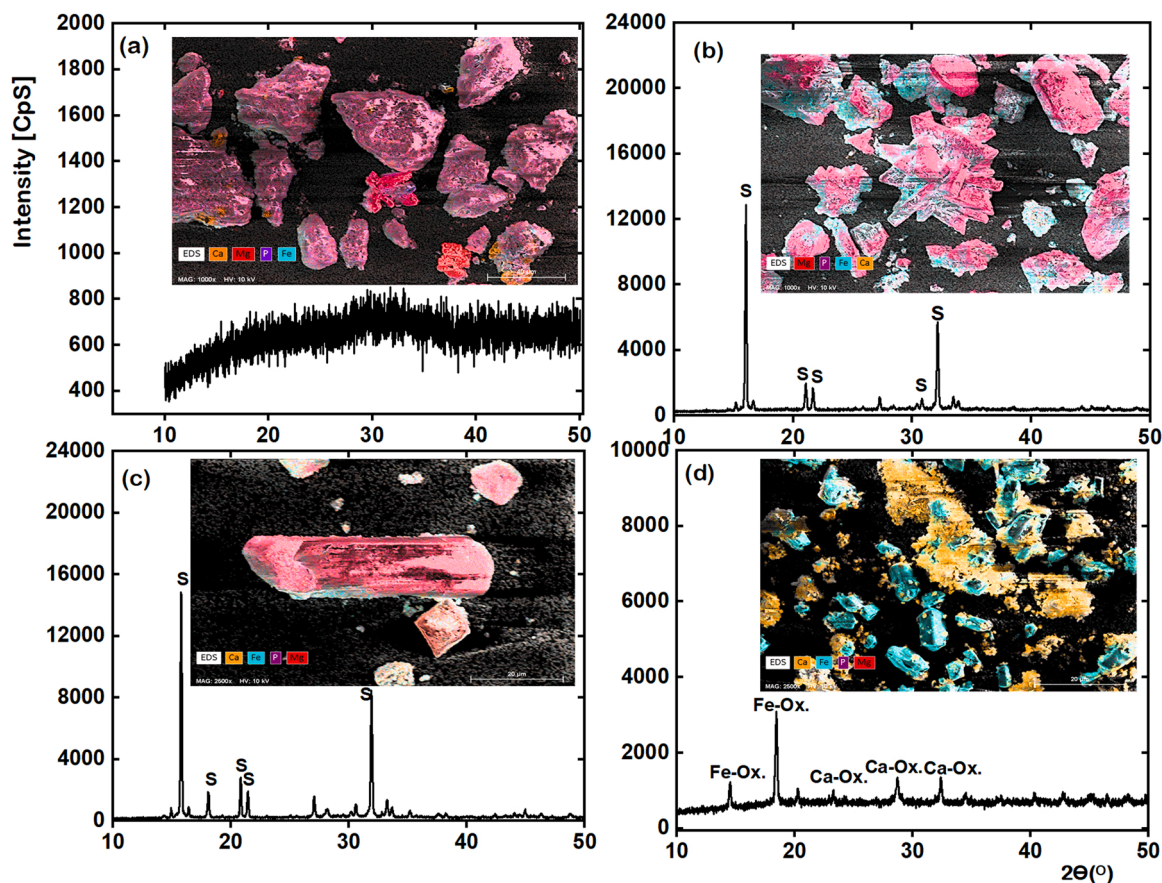


Fig. 3. XRD and SEM-EDS graphs of recovered salts from the HTC liquor (a), struvite (s) precipitation without iron removal (b), and after iron removal (c), and the extraction residue with iron oxalate (Fe-ox.) and calcium oxalate (Ca-ox.) (d).

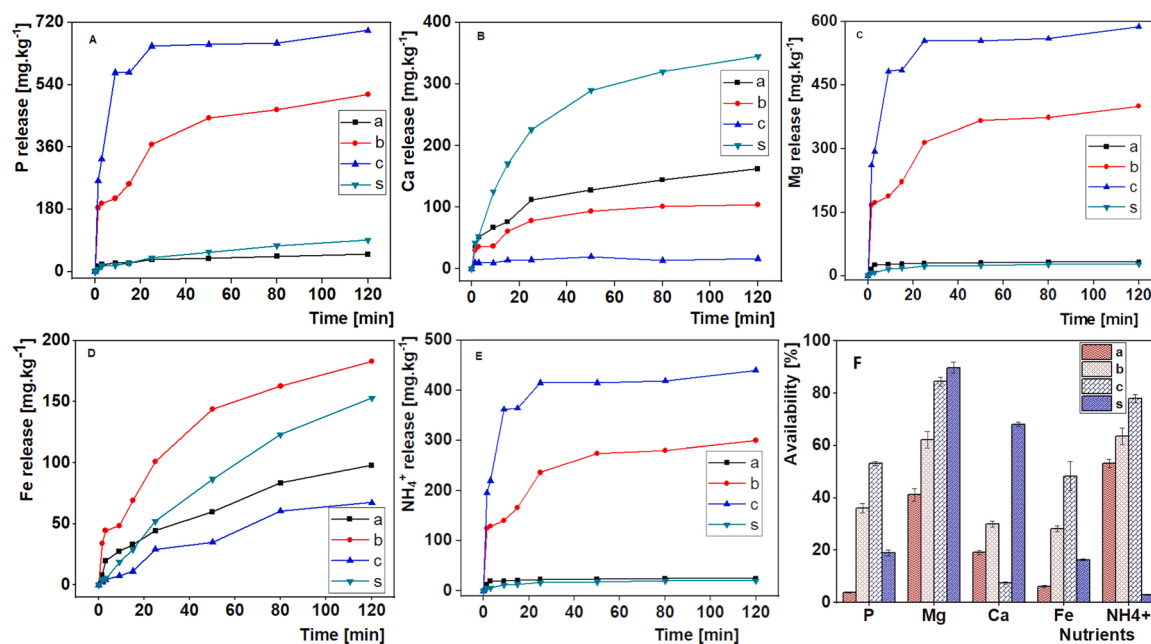


Fig. 4. In vitro nutrient release assay in citrate solution for phosphorus (A), calcium (B), magnesium (C), iron (D), ammonium (E), and their availability (F).

mitigated by P extraction for iron removal followed by struvite precipitation from the extract (c and c' in Table 4). By applying the optimum dosage on the P extract, the product iron content was less than 2%, the P content was up to 28.18% and 31% obtained experimentally on real

(product c) and artificial (product c') samples, respectively. The products comply with the European regulation 2019/1009 regarding the market for phosphorus fertilizers [38].

The used combination of extraction with oxalic acid and struvite

Table 5

Kinetic parameters of the in-vitro nutrient release assay for recovered products (a, b, c) and their raw sludge (s).

Model	Product	$C_{max}[mgkg^{-1}]$	$k [min^{-1}]$	R^2	τ	t_{80}	Availability [%]
P release	a	46.42 ± 2.59	0.04 ± 0.01	0.894	22.50 ± 5.38	36.22 ± 8.65	3.77 ± 0.21
	b	497.08 ± 25.13	0.04 ± 0.01	0.92	23.72 ± 4.94	38.18 ± 7.94	36.03 ± 1.82
	c	653.32 ± 10.35	0.23 ± 0.02	0.981	4.28 ± 0.41	6.88 ± 0.65	53.10 ± 0.84
	s	108.39 ± 7.07	0.01 ± 0.00	0.988	69.39 ± 9.53	111.67 ± 15.3	18.96 ± 1.24
Mg Release	a	30.49 ± 0.54	0.55 ± 0.06	0.965	1.84 ± 0.19	2.95 ± 0.31	41.20 ± 2.34
	b	387.63 ± 19.21	0.05 ± 0.01	0.899	18.68 ± 4.19	30.06 ± 6.74	62.22 ± 3.09
	c	547.92 ± 10.55	0.27 ± 0.03	0.968	3.68 ± 0.44	5.93 ± 0.70	84.42 ± 1.63
	s	25.81 ± 0.60	0.08 ± 0.01	0.975	12.16 ± 1.25	19.58 ± 2.01	89.78 ± 2.09
Ca release	a	153.47 ± 5.85	0.04 ± 0.01	0.958	23.44 ± 3.45	37.73 ± 5.55	19.09 ± 0.76
	b	102.80 ± 3.73	0.05 ± 0.01	0.956	20.31 ± 2.97	32.69 ± 4.79	29.97 ± 1.12
	c	14.82 ± 0.77	0.41 ± 0.14	0.760	2.42 ± 0.79	3.90 ± 1.27	7.45 ± 0.39
	s	335.40 ± 4.26	0.04 ± 0.00	0.996	22.76 ± 1.02	36.63 ± 1.64	68.16 ± 0.87
Fe release	a	109.87 ± 7.61	0.02 ± 0.00	0.979	59.67 ± 9.65	96.04 ± 15.5	6.13 ± 0.42
	b	187.91 ± 7.61	0.03 ± 0.00	0.979	38.12 ± 4.68	61.36 ± 7.53	28.26 ± 1.14
	c	90.83 ± 10.51	0.01 ± 0.00	0.979	83.93 ± 17.5	135 ± 28.5	48.31 ± 5.59
	s	210.37 ± 4.65	0.01 ± 0.00	0.999	91.78 ± 3.49	147.71 ± 5.62	16.34 ± 0.36
NH_4^+ release	a	22.86 ± 0.41	0.55 ± 0.06	0.965	1.84 ± 0.19	2.95 ± 0.31	53.16 ± 1.56
	b	290.72 ± 14.41	0.05 ± 0.01	0.899	18.68 ± 4.19	30.06 ± 6.74	63.61 ± 3.16
	c	410.94 ± 7.91	0.27 ± 0.03	0.968	3.68 ± 0.44	5.93 ± 0.70	77.98 ± 1.51
	s	19.36 ± 0.45	0.08 ± 0.01	0.975	12.16 ± 1.25	19.58 ± 2.01	2.92 ± 0.07

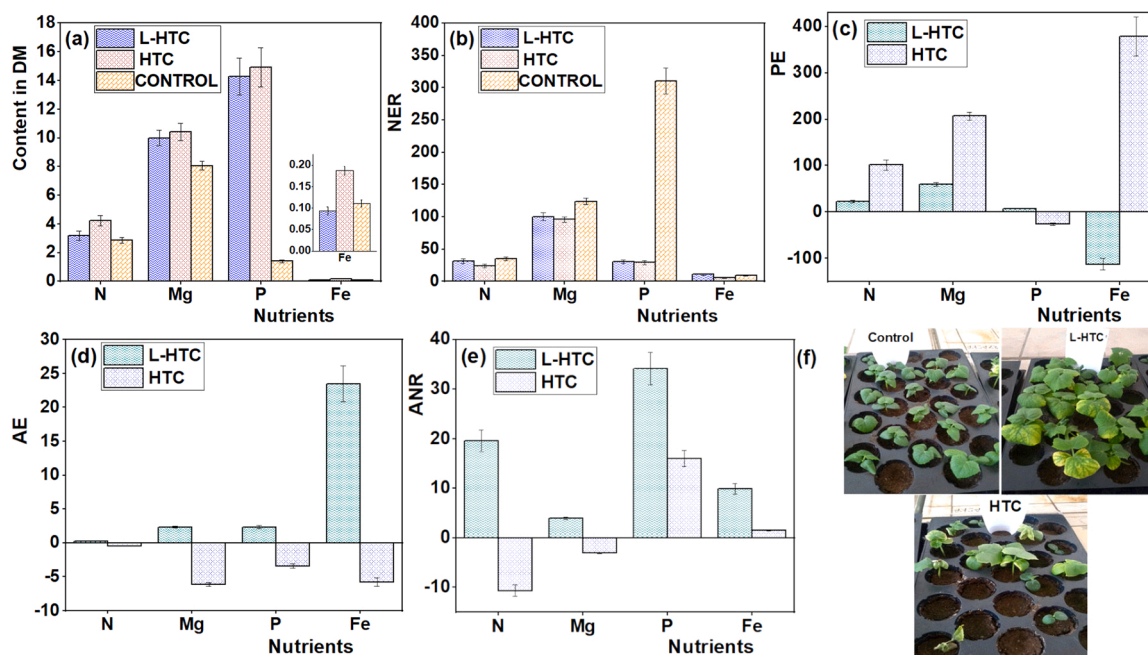


Fig. 5. Nutrient content (a) on the basis of dry biomass for N (%), and other elements ($g \cdot kg^{-1}$); their use efficiency parameters: (b) NER ($kg DM \cdot kg^{-1}$); (c) PE in kg net DM yield per unit mass of nutrient uptake; (d) AE as kg net DM per unit mass of applied nutrient; (e) ANR as the % of uptake by net DM on the unit mass of applied nutrient, and (f) the plant status for control, fertilized soil by struvite with (L-HTC) and without (HTC) iron removal.

precipitation is a beneficial process for its ability to recover iron and P into two separate and valuable products. Struvite, thereby recovered, is used as an efficient P fertilizer. In contrast, the extraction solid product of iron (II) and calcium oxalates have been reported for further use, either as sorbent material or as carbonate salts after their thermo-treatment [66]. In particular, ferrous oxalate is a useful product member of metal organic framework polymers [67]. The elemental characterization of recovered products is presented in Table 4.

The XRD characterization of the precipitates indicates various aspects of the crystallinity of the recovered products. The direct precipitation at pH 9 leads to the production of amorphous salts. The predominant products are iron phosphate and calcium phosphate following their high concentration in the liquor, their decrease in precipitation effluent, and their high concentration in the products. This is highlighted by their SEM-EDS images showing the elemental mapping

on the material surface (Fig. 3.a), and their products' analytical results (Table 4, products a and a'). In contrast, the struvite rich products were produced at optimum dosage and exhibited closer crystal lattice parameters with a struvite pattern. For those products, the crystal lattice parameters a: 6.955 , b: 6.142 , and c: 11.218 \AA for struvite crystals were observed, and the characteristic peaks were at 15.9 , 20.8 , 21.5 , and $31-32 \text{ \Theta}$. The XRD spectra of the products are presented in Fig. 3.a-d in which the struvite pattern is marked by the letter S. The same struvite crystal properties were identified in specific works by Whitaker et al. [68], thus highlighting the achieved struvite predominance in the products [68].

Furthermore, microscopic images correlate with XRD results. In addition to the lower intensity caused by the formation of amorphous phosphate salts, the SEM-EDS image in Fig. 3.a indicates a non-crystalline structure with calcium phosphate as the major element

with high signal on the product surface elemental mapping. The results improve in Fig. 3.b after addition of magnesium salts.

The higher XRD intensity and best crystal structures are obtained after P extraction and iron removal. In this case, the big portion of P is precipitated as struvite (Fig. 3c). On the other hand, the solid phase obtained through extraction is an iron and calcium product of the oxalate solid mixture. Its XRD diffraction shows lower peak intensity, while the SEM-EDS indicates high iron and calcium on surface elemental mapping (Fig. 3.d). The responsible products are their oxalates salts. They are materials with orthorhombic shapes and their structures were confirmed by XRD analysis.

3.6. Fertilizer quality

The in vitro nutrient release assay in 2% citric acid solution demonstrated a significant difference in P release and availability. The P purification from the sludge liquor by extraction followed by precipitation demonstrated the advantage in nutrients availability. The in-vitro nutrient release assay is presented in Fig. 4.

The P release in terms of C_{\max} for the raw sludge (s) was lower than their purified products. The product (c) of P extraction combined with precipitation exhibits better nutrient availability with higher C_{\max} than others. This property is affected by increased iron and calcium content, where C_{\max} was lower in precipitation products obtained without iron removal (a, b). The effect was even stronger in the case of HTC liquor recovered salts, where P release was the lowest of phosphate precipitates (Fig. 4a). Nutrient availability was more decreased with a lower level of struvite content, and high iron and calcium content. The latter reached a higher concentration of release in citric acid for products a, b, and s. In particular, for P and N availability, the product c of P extract reached the highest percentage of solubility in citric acid solution (Fig. 4F and Table 5).

The *in-vivo* assay on the cucumber demonstrated similar effects. The germination test showed a difference in terms of plant health and nutrient effects.

After one week, the seeds were effectively germinated at 80%, 32%, and 88% for the control, and the soil fertilized with P products b and c, respectively. The lower germination rate observed for high iron content products (b) highlights the risk of phyto-toxicity. On the other hand, removing a large fraction of iron makes the product more valuable for fertilizer application. The Iron content in the product is within the accepted range and becomes a benefit to the plant for the production of a micronutrient bio-fortified diet. After two weeks, the harvested fresh biomass was weighed, dried, and analyzed on a dry matter basis.

With consideration of nutrient efficiency ratio, the NER parameter is lower for fertilized biomass than the control, thus highlighting the higher uptake of nutrients in the fertilized trials. The comparative experiments were aimed at highlighting the effect of iron on fertilizer quality. The high efficiency parameters were found with product c (L-HTC), the product after iron removal. On the other hand, the efficiency parameters decreased on trials fertilized with b (HTC) due to an excess of iron content. This observation is an emphasis on iron content limitation in phosphate fertilizers. Additionally, this negative effect was studied and confirmed elsewhere [21]. Nevertheless, the iron optimum content in the product demonstrated the improvement of AE and ANR parameter. The latter became worse for trials fertilized with high iron content where they became negative, thus the applied nutrients remained almost unused compared to the control trial. In contrast, the PE results demonstrate the potential of micro-elements in plant growth, where the

PE was improved. Similar effects were previously reported by other research where iron was particularly the major micro-element in the fertilizer formulation [69]. This plays a major role in the bio-fortification and the production of micronutrients-based functional foods. In addition, previous research found that application of 2.5 g struvite per kg of soil increased the amount of cucumber harvested plant biomass by 64% versus control treatment [70]. The nutrients use efficiency parameters that include NER, PE, AE, and ANR for Eqs. (3–6) are reported in Fig. 5.a–e.

Supplementary materials connected to this work include detailed data on nutrient release, use efficiency, cost estimation and DOEs.

4. Conclusion

The P-rich sludge produced chemically with ferric coagulants can be used for iron, and P recycling. The HTC processing of sludge produced hydrochar which is a carbon and energy dense material, while the liquor was used in this work to recover the dissolved P. Due to the high iron concentration in the liquor, the product of direct precipitation contains a high amount of iron that limits its use as phosphate fertilizer. The P extraction with oxalic acid $0.375 \text{ mol}\cdot\text{L}^{-1}$ was effective for P extraction and iron removal prior to struvite precipitation. The process conditions that include pH 9, and mixing Mg: P and NH_4^+ : P mole ratios of 1.73 and 1.14, respectively, allow producing a micro-element based green crystal fertilizer. The product complies with regulations, and has demonstrated good in-vitro nutrient availability and in vivo efficient nutrient uptake by plants. The P and iron are efficiently removed and reach an effluent concentration $< 2 \text{ mg}\cdot\text{L}^{-1}$. Ammonium in the effluent was slightly higher than the accepted limit. Its sorption by clinoptilolite makes it falls within acceptable limits. Furthermore, iron and calcium oxalate obtained during extraction can be used in different chemical applications, including nanomaterial production, siderite synthesis, or coagulants. The HTC conditions treated the sludge into hydrochar with lower P dissolution rate in the liquor. The future trends include studying favorable conditions for P dissolution in the HTC liquor and full scale cost-evaluation for struvite precipitation.

CRedit authorship contribution statement

Claver Numviyimana: Conceptualization, Methodology and Writing – original draft. **Jolanta Warchol:** Supervision, Reviewing and Editing. **Nidal Kalhaf:** Data curation, sampling and sample processing. **James J Leahy:** Supervision. **Katarzyna Chojnacka:** Conceptualization, Supervision, reviewing and editing.

Declaration of Competing Interest

The authors declare that they have no known competing financial interests or personal relationships that could have appeared to influence the work reported in this paper.

Acknowledgement

We thank Dr Katarzyna Winiarska, Ms. Sylwia Basladynska, and Ms. Paulina Jagodka for laboratory support. This work was financially supported by European Union's Horizon 2020 research and innovation programme under the Marie Skłodowska-Curie Actions, grant agreement number 814258.

Appendix A. DOE and optimum results of precipitation

run	Factors			Yield without EP*				Yield with PE			
	pH	Mg:P (mol.mol ⁻¹)	N:P	RecP (%)	RecN (g/100 ml)	X-NH ₄ ⁺ (%)	Q _e (mg.g ⁻¹)	RecP (%)	RecN (g/100 ml)	X-NH ₄ ⁺ (%)	Q _e (mg.g ⁻¹)
1	7.5	1.0	0.7	94.30	0.58	6.33	0.72	82.50	0.30	5.71	0.28
2	10.5	1.5	0.2	99.50	0.11	0.06	1.12	96.90	0.09	0.86	0.00
3	9.0	1.0	0.2	95.50	0.17	1.69	0.46	86.00	0.09	1.13	0.01
4	9.0	1.0	1.2	99.80	0.85	6.60	2.37	94.90	0.48	6.31	0.83
5	10.5	2.0	0.7	99.90	0.52	1.73	1.21	99.40	0.29	4.50	0.47
6	9.0	1.5	0.7	99.80	0.42	6.28	1.94	94.60	0.32	6.21	0.85
7	7.5	1.5	1.2	96.70	0.91	7.34	1.75	90.60	0.51	6.38	0.60
8	7.5	1.5	0.2	90.90	0.15	1.95	1.73	81.20	0.08	1.69	0.25
9	9.0	1.5	0.7	99.70	0.40	6.53	2.08	93.60	0.32	6.11	0.85
10	9.0	2.0	0.2	97.10	0.16	1.94	1.58	93.70	0.10	1.12	0.00
11	9.0	2.0	1.2	99.70	0.89	6.66	2.16	98.40	0.47	6.34	1.64
12	10.5	1.0	0.7	99.20	0.54	3.37	1.84	98.40	0.31	4.62	0.01
13	7.5	2.0	0.7	95.40	0.39	7.05	2.18	86.60	0.29	5.39	1.04
14	9.0	1.5	0.7	99.50	0.42	6.32	1.82	94.00	0.31	6.21	0.85
15	10.5	1.5	1.2	99.90	0.79	3.37	2.52	99.50	0.50	5.91	1.00
Experimental model parameters											
Intercept				-8.330	2.560	-58.300	1.950	-59.00	-0.388	-21.500	-10.60
A-pH				17.900	-0.351	11.700	0.040	21.82	0.050	3.960	2.18
B-Mg:P				10.200	-1.320	11.300	0.217	23.42	0.187	5.700	2.33
C-NH ₄ ⁺ :P				28.100	0.668	21.200	0.488	34.32	0.563	14.400	-1.62
AB				-0.122	0.058	-0.786	-0.521	-1.07	-0.005	0.069	-0.10
AC				-1.830	-0.029	-0.694	0.346	-2.25	-0.006	0.122	0.22
BC				-1.700	0.042	-0.192	-0.333	-4.17	-0.013	0.041	0.82
A ²				-0.817	0.016	-0.623	-0.161	-0.79	-0.002	-0.246	-0.12
B ²				-2.370	0.242	-1.420	-0.300	-2.25	-0.047	-2.150	-0.49
C ²				-4.190	0.173	-7.190	-0.009	-1.04	-0.064	-7.530	-0.43
p-Value				<0.001	<0.001	<0.001	<0.001	<0.001	<0.001	<0.001	0.035
F				72.3	38.7	45.9	14.7	36	196	255	5.63
R ²				0.992	0.986	0.988	0.963	0.985	0.997	0.998	0.91
P-lack fit				0.058	0.017	0.0501	0.272	0.0825	0.0935	0.0684	-
Precision				27.9	17	21.6	13.3	19.52	37.2	42.2	9.08
Optimum factors level				Ca:P 0.25** pH = 9.0, Mg:P = 1.4, N:P = 1.14				pH = 9.0, Mg:P = 1.73, N:P = 1.14,			
Optimum pred. yields				RecP = 100 ± 0.13, RecN = 0.761, X-NH ₄ ⁺ = 7.01 ± 0.15, Q _e = 2.37, D = 0.964				RecP = 97 ± 0.41%, RecN = 0.467, X-NH ₄ ⁺ = 6.76 ± 0.06, Q _e = 1.35, D = 0.951			
Experimental yields				RecP = 99.96 ± 0.22, RecN = 0.768, X-NH ₄ ⁺ = 6.76 ± 0.15				RecP = 99.96 ± 0.46%, RecN = 0.502, X-NH ₄ ⁺ = 7.28 ± 0.05, Q _e = 1.25			

EP* = P extraction, Ca:P** was adjusted by additional K₂HPO₄.

Appendix B. Supporting information

Supplementary data associated with this article can be found in the online version at [doi:10.1016/j.jece.2021.106947](https://doi.org/10.1016/j.jece.2021.106947).

References

- T.Z.X. Lal R., K.D. Wiebe, Global soil nutrient depletion and yield reduction, *J. Sustain. Agric.* 26 (2005) 123–146, https://doi.org/10.1300/J064v26n01_10.
- A. Amann, O. Zoboli, J. Krampe, H. Rechberger, M. Zessner, L. Egle, Environmental impacts of phosphorus recovery from municipal wastewater, *Resour. Conserv. Recycl.* 130 (2018) 127–139, <https://doi.org/10.1016/j.resconrec.2017.11.002>.
- S. Kolev, General characteristics and treatment possibilities of dairy wastewater – a review, *Food Technol. Biotechnol.* 53 (2017) 237–242, <https://doi.org/10.17113/ft>.
- S.M. Ashekuzzaman, P. Forrestal, K. Richards, O. Fenton, Dairy industry derived wastewater treatment sludge: generation, type and characterization of nutrients and metals for agricultural reuse, *J. Clean. Prod.* 230 (2019) 1266–1275, <https://doi.org/10.1016/j.jclepro.2019.05.025>.
- P. Izadi, P. Izadi, A. Eldyasti, Design, operation and technology configurations for enhanced biological phosphorus removal (EBPR) process: a review, *Rev. Environ. Sci. Bio Technol.* 19 (2020) 561–593, <https://doi.org/10.1007/s11157-020-09538-w>.
- EIP-AGRI, EIP-AGRI Focus Group. Nutrient Recycling, 2017. (https://ec.europa.eu/eip/agriculture/sites/default/files/eip-agri_fg_nutrients_recycling_final_report_2017_en.pdf).
- K. Nadeem, M. Alliet, Q. Plana, J. Bernier, S. Azimi, V. Rocher, C. Albasi, Modeling, simulation and control of biological and chemical P-removal processes for membrane bioreactors (MBRs) from lab to full-scale applications: State of the art, *Sci. Total Environ.* (2021), 151109, <https://doi.org/10.1016/j.scitotenv.2021.151109>.
- Y. Lei, Z. Zhan, M. Saakes, R.D. van der Weijden, C.J.N. Buisman, Electrochemical recovery of phosphorus from acidic cheese wastewater: feasibility, quality of products, and comparison with chemical precipitation, *ACS ES&T Water* 1 (2021) 1002–1013, <https://doi.org/10.1021/acsestwater.0c00263>.
- J.T. Bunce, E. Ndam, I.D. Ofiteru, A. Moore, D.W. Graham, A review of phosphorus removal technologies and their applicability to small-scale domestic wastewater treatment systems, *Front. Environ. Sci.* 6 (2018) 1–15, <https://doi.org/10.3389/fenvs.2018.00008>.
- T. Prot, W. Wijdeveld, L.E. Eshun, A.I. Dugulan, K. Goubitz, L. Korving, M.C.M. Van Loosdrecht, Full-scale increased iron dosage to stimulate the formation of vivianite and its recovery from digested sewage sludge, *Water Res.* 182 (2020), 115911, <https://doi.org/10.1016/j.watres.2020.115911>.
- I. Takács, S. Murthy, S. Smith, M. McGrath, Chemical phosphorus removal to extremely low levels: experience of two plants in the Washington, DC area, *Water Sci. Technol.* 53 (2006) 21–28, <https://doi.org/10.2166/wst.2006.402>.
- R.R.Z. Tarpani, C. Alfonsín, A. Hospido, A. Azapagic, Life cycle environmental impacts of sewage sludge treatment methods for resource recovery considering ecotoxicity of heavy metals and pharmaceutical and personal care products, *J. Environ. Manag.* 260 (2020), 109643, <https://doi.org/10.1016/j.jenvman.2019.109643>.
- D.P. Smyth, A.L. Fredeen, A.L. Booth, Reducing solid waste in higher education: The first step towards “greening” a university campus, *Resour. Conserv. Recycl.* 54 (2010) 1007–1016, <https://doi.org/10.1016/j.resconrec.2010.02.008>.
- EurEau, Briefing Note Waste Water Treatment - Sludge Management, 2021. (<https://www.eureau.org/resources/briefing-notes/5629-briefing-note-on-sludge-management/file>).
- A. Akhiar, A. Battimelli, M. Torrijos, H. Carrere, Comprehensive characterization of the liquid fraction of digestates from full-scale anaerobic co-digestion, *Waste Manag.* 59 (2017) 118–128, <https://doi.org/10.1016/j.wasman.2016.11.005>.

- [16] Y. Tian, L. Cui, Q. Lin, G. Li, X. Zhao, The sewage sludge biochar at low pyrolysis temperature had better improvement in urban soil and turf grass, *Agronomy* 9 (2019), <https://doi.org/10.3390/agronomy9030156>.
- [17] L. Egle, H. Rechberger, J. Krampe, M. Zessner, Phosphorus recovery from municipal wastewater: an integrated comparative technological, environmental and economic assessment of P recovery technologies, *Sci. Total Environ.* 571 (2016) 522–542, <https://doi.org/10.1016/j.scitotenv.2016.07.019>.
- [18] S. Tavazzi, G. Locoro, S. Comerio, E. Sobiecka, R. Loos, O. Gans, M. Ghiani, G. Umlauf, G. Suurkuusk, B. Paracchini, C. Cristache, I. Fissiaux, A.A. Riuz, B.M. Gawlik, Occurrence and levels of selected compounds in European sewage sludge samples (FATE SEES), *Ec.Europa.Eu/Jrc/Sites/Default/Files*, 2012. (<https://doi.org/10.2788/67153>).
- [19] K. Fijalkowski, A. Rorat, A. Grobelak, M.J. Kacprzak, The presence of contaminations in sewage sludge – the current situation, *J. Environ. Manag.* 203 (2017) 1126–1136, <https://doi.org/10.1016/j.jenvman.2017.05.068>.
- [20] W. Shi, M.G. Healy, S.M. Ashekuzzaman, K. Daly, J.J. Leahy, O. Fenton, Dairy processing sludge and co-products: a review of present and future re-use pathways in agriculture, *J. Clean. Prod.* 314 (2021), 128035, <https://doi.org/10.1016/j.jclepro.2021.128035>.
- [21] W. Römer, I.F. Samie, Iron-rich sewage sludge is not suitable for phosphorus recycling in agriculture, *Wasser Und Boden* 54 (2002) 28–32. (https://www.researchgate.net/publication/289434163_Iron-rich_sewage_sludge_is_not_suitable_for_phosphorus_recycling_in_agriculture).
- [22] H. Kahiluoto, M. Kuisma, E. Ketoja, T. Salo, J. Heikkinen, Phosphorus in manure and sewage sludge more recyclable than in soluble inorganic fertilizer, *Environ. Sci. Technol.* 49 (2015) 2115–2122, <https://doi.org/10.1021/es503387y>.
- [23] S.M. Ashekuzzaman, P. Forrester, K.G. Richards, K. Daly, O. Fenton, Grassland phosphorus and nitrogen fertiliser replacement value of dairy processing dewatered sludge, *Sustain. Prod. Consum.* 25 (2021) 363–373, <https://doi.org/10.1016/j.spc.2020.11.017>.
- [24] A. Gianico, C. Braguglia, A. Gallipoli, D. Montecchio, G. Mininni, Land application of biosolids in Europe: possibilities, constraints and future perspectives, *Water* 13 (2021) 103, <https://doi.org/10.3390/w13010103>.
- [25] E. Atallah, W. Kwapinski, M.N. Ahmad, J.J. Leahy, J. Zeaiter, Effect of water-sludge ratio and reaction time on the hydrothermal carbonization of olive oil mill wastewater treatment: Hydrochar characterization, *J. Water Process Eng.* 31 (2019), 100813, <https://doi.org/10.1016/j.jwpe.2019.100813>.
- [26] B.M. Ghanim, W. Kwapinski, J.J. Leahy, Hydrothermal carbonisation of poultry litter: Effects of initial pH on yields and chemical properties of hydrochars, *Bioresour. Technol.* 238 (2017) 78–85, <https://doi.org/10.1016/j.biortech.2017.04.025>.
- [27] D. Bhatt, A. Shrestha, R.K. Dahal, B. Acharya, P. Basu, R. MacEwen, Hydrothermal carbonization of biosolids from Waste water treatment plant, *Energies* 11 (2018) 1–10, <https://doi.org/10.3390/en11092286>.
- [28] O.P. Crossley, R.B. Thorpe, D. Peus, J. Lee, Phosphorus recovery from process waste water made by the hydrothermal carbonisation of spent coffee grounds, *Bioresour. Technol.* 301 (2020), 122664, <https://doi.org/10.1016/j.biortech.2019.122664>.
- [29] S. Daneshgar, A. Callegari, A.G. Capodaglio, D. Vaccari, The potential phosphorus crisis: Resource conservation and possible escape technologies: a review, *Resources* 7 (2018), <https://doi.org/10.3390/resources7020037>.
- [30] W. Kwapinski, C.M.P. Byrne, E. Kryachko, P. Wolfram, C. Adley, J.J. Leahy, E. H. Novotny, M.H.B. Hayes, Biochar from biomass and waste, *Waste Biomass Valoriz.* 1 (2010) 177–189, <https://doi.org/10.1007/s12649-010-9024-8>.
- [31] W. Shi, O. Fenton, S.M. Ashekuzzaman, K. Daly, J.J. Leahy, N. Khalaf, Y. Hu, K. Chojnacka, C. Numviyimana, M.G. Healy, An examination of maximum legal application rates of dairy processing and associated STRUBIAS fertilising products in agriculture, *J. Environ. Manag.* 301 (2022), 113880, <https://doi.org/10.1016/j.jenvman.2021.113880>.
- [32] A. Siciliano, C. Limonti, S. Mehariya, A. Molino, V. Calabrò, Biofuel production and phosphorus recovery through an integrated treatment of agro-industrial waste, *Sustainability* 11 (2018) 1–17, <https://doi.org/10.3390/su11010052>.
- [33] L.C. Bell, H. Mika, B.J. Kruger, Synthetic hydroxyapatite-solubility product and stoichiometry of dissolution, *Arch. Oral Biol.* 23 (1978) 329–336, [https://doi.org/10.1016/0003-9969\(78\)90089-4](https://doi.org/10.1016/0003-9969(78)90089-4).
- [34] C. Kazadi Mbamba, S. Tait, X. Flores-Alsina, D.J. Batstone, A systematic study of multiple minerals precipitation modelling in wastewater treatment, *Water Res.* 85 (2015) 359–370, <https://doi.org/10.1016/j.watres.2015.08.041>.
- [35] R. Priambodo, Y.J. Shih, Y.H. Huang, Phosphorus recovery as ferrous phosphate (vivianite) from wastewater produced in manufacture of thin film transistor-liquid crystal displays (TFT-LCD) by a fluidized bed crystallizer (FBC), *RSC Adv.* 7 (2017) 40819–40828, <https://doi.org/10.1039/c7ra06308c>.
- [36] M. Hanhoun, L. Montastruc, C. Azzaro-Pantel, B. Biscans, M. Frèche, L. Pibouveau, Temperature impact assessment on struvite solubility product: a thermodynamic modeling approach, *Chem. Eng. J.* 167 (2011) 50–58, <https://doi.org/10.1016/j.cej.2010.12.001>.
- [37] S.M. Heilmann, J.S. Molde, J.G. Timler, B.M. Wood, A.L. Mikula, G.V. Vozhdavey, E.C. Colosky, K.A. Spokas, K.J. Valentas, Phosphorus reclamation through hydrothermal carbonization of animal manures, *Environ. Sci. Technol.* 48 (2014) 10323–10329, <https://doi.org/10.1021/es501872k>.
- [38] EU, Regulation (EU) 2019/1009 of the European Parliament and of the Council of 5 June 2019 laying down rules on the making available on the market of EU fertilising products and amending Regulation (EC) No 1069/2009 and (EC) No 1107/2009 and repealing Regulation, *Off. J. Eur. Union.* 2019 (2019) 1–114. (<https://eur-lex.europa.eu/legal-content/EN/TXT/PDF/?uri=CELEX:32019R1009&from=EN>).
- [39] L. Egle, H. Rechberger, M. Zessner, Overview and description of technologies for recovering phosphorus from municipal wastewater, *Resour. Conserv. Recycl.* 105 (2015) 325–346, <https://doi.org/10.1016/j.resconrec.2015.09.016>.
- [40] H. Elomaa, S. Seisko, J. Lehtola, M. Lundström, A study on selective leaching of heavy metals vs. iron from fly ash, *J. Mater. Cycles Waste Manag.* 21 (2019) 1004–1013, <https://doi.org/10.1007/s10163-019-00858-w>.
- [41] A. Verma, R. Kore, D.R. Corbin, M.B. Shifflett, Metal recovery using oxalate chemistry: a technical review, *Ind. Eng. Chem. Res.* 58 (2019) 15381–15393, <https://doi.org/10.1021/acs.iecr.9b02598>.
- [42] Q. Wang, C. Zhang, D. Patel, H. Jung, P. Liu, B. Wan, S.G. Pavlostathis, Y. Tang, Coevolution of iron, phosphorus, and sulfur speciation during anaerobic digestion with hydrothermal pretreatment of sewage sludge, *Environ. Sci. Technol.* 54 (2020) 8362–8372, <https://doi.org/10.1021/acs.est.0c00501>.
- [43] M. Ahmed, L.S. Lin, Ferric reduction in organic matter oxidation and its applicability for anaerobic wastewater treatment: a review and future aspects, *Rev. Environ. Sci. Biotechnol.* 16 (2017) 273–287, <https://doi.org/10.1007/s11157-017-9424-3>.
- [44] S. Vudagandla, N. Siva Kumar, V. Dharmendra, M. Asif, V. Balam, H. Zhengxu, Z. Zhen, Determination of boron, phosphorus, and molybdenum content in biosludge samples by microwave plasma atomic emission spectrometry (MP-AES), *Appl. Sci.* 7 (2017) 264, <https://doi.org/10.3390/app7030264>.
- [45] E.V. Musvoto, M.C. Wentzel, R.E. Loewenthal, G.A. Ekama, Integrated chemical-physical processes modelling - I. Development of a kinetic-based model for mixed weak acid/base systems, *Water Res.* 34 (2000) 1857–1867, [https://doi.org/10.1016/S0043-1354\(99\)00334-6](https://doi.org/10.1016/S0043-1354(99)00334-6).
- [46] M. Marinoni, J. Carrayrou, Y. Lucas, P. Ackerer, Thermodynamic equilibrium solutions through a modified Newton Raphson method, *AIChE J.* 63 (2017) 1246–1262, <https://doi.org/10.1002/aic.15506>.
- [47] P. Nancollas, G.H. Amjad, Z. Koutsoukos, Calcium phosphates—speciation, solubility, and kinetic considerations, *Chem. Model. Aqueous Syst.* (1979) 475–497, <https://doi.org/10.1021/bk-1979-0093.ch023>.
- [48] I.D.A.A. Warmadewanthi, M.A. Zulkarnain, N. Ikhlas, S.B. Kurniawan, S.R. S. Abdullah, Struvite precipitation as pretreatment method of mature landfill leachate, *Bioresour. Technol.* 15 (2021), 100792, <https://doi.org/10.1016/j.biortech.2021.100792>.
- [49] R.I. Gelb, Conductometric determination of pKa values—oxalic and squaric acids, *Anal. Chem.* 43 (1971) 1110–1113, <https://doi.org/10.1021/ac60303a028>.
- [50] O. Mekmene, S. Quillard, T. Rouillon, J.M. Boulter, M. Piot, F. Gaucheron, Effects of pH and Ca/P molar ratio on the quantity and crystalline structure of calcium phosphates obtained from aqueous solutions, *Dairy Sci. Technol.* 89 (2009) 301–316, <https://doi.org/10.1051/dst/2009019>.
- [51] S. Shaddel, T. Grini, S. Ucar, K. Azrague, J.P. Andreassen, S.W. Østerhus, Struvite crystallization by using raw seawater: Improving economics and environmental footprint while maintaining phosphorus recovery and product quality, *Water Res.* 173 (2020), 115572, <https://doi.org/10.1016/j.watres.2020.115572>.
- [52] C. Numviyimana, J. Warchol, G. Izdorzcyk, S. Baśladyńska, K. Chojnacka, Struvite production from dairy processing wastewater: Optimizing reaction conditions and effects of foreign ions through multi-response experimental models, *J. Taiwan Inst. Chem. Eng.* 117 (2020) 182–189, <https://doi.org/10.1016/j.jtice.2020.11.031>.
- [53] M.A. de Boer, M. Hammerton, J.C. Sloop, Uptake of pharmaceuticals by sorbent-amended struvite fertilisers recovered from human urine and their bioaccumulation in tomato fruit, *Water Res.* 133 (2018) 19–26, <https://doi.org/10.1016/j.watres.2018.01.017>.
- [54] A. Kotoulas, D. Agathou, I. Triantaphyllidou, T. Tatoulis, C. Kratos, A. Tekerlekopoulou, D. Vayenas, Zeolite as a potential medium for ammonium recovery and second choice whey treatment, *Water* 11 (2019) 136, <https://doi.org/10.3390/w11010136>.
- [55] D. Kim, K.J. Min, K. Lee, M.S. Yu, K.Y. Park, Effects of pH, molar ratios and pretreatment on phosphorus recovery through struvite crystallization from effluent of anaerobically digested swine wastewater, *Environ. Eng. Res.* 22 (2017) 12–18, <https://doi.org/10.4491/eer.2016.037>.
- [56] R. Bashar, K. Gungor, K.G. Karthikeyan, P. Barak, Cost effectiveness of phosphorus removal processes in municipal wastewater treatment, *Chemosphere* 197 (2018) 280–290, <https://doi.org/10.1016/j.chemosphere.2017.12.169>.
- [57] M. Moh, T. Zin, D. Tiwari, D. Kim, Maximizing ammonium and phosphate recovery from food wastewater and incinerated sewage sludge ash by optimal Mg dose with RSM, *J. Ind. Eng. Chem.* 86 (2020) 136–143, <https://doi.org/10.1016/j.jiec.2020.02.020>.
- [58] W.O. Santos, E.M. Mattiello, M.S.C. Barreto, R.B. Cantarutti, Acid ammonium citrate as P extractor for fertilizers of varying solubility, *Rev. Bras. Ciência Do Solo* 43 (2019) 1–12, <https://doi.org/10.1590/18069657rbs20180072>.
- [59] C. Ramprasad, D. Alekha, C. Bhismita, S.C. Deepika, Precipitation of struvite by sustainable waste materials and use as slow release fertilizer—a circular economy approach, *IOP Conf. Ser. Mater. Sci. Eng.* 955 (2020), <https://doi.org/10.1088/1757-899X/955/1/012088>.
- [60] V.C. Baligar, N.K. Fageria, Z.L. He, Nutrient use efficiency in plants, *Commun. Soil Sci. Plant Anal.* 32 (2001) 921–950, <https://doi.org/10.1081/CSS-100104098>.
- [61] S.S. Dalahmeh, Y. Stenström, M. Jebrane, L.D. Hylander, G. Daniel, I. Heinmaa, Efficiency of iron- and calcium-impregnated biochar in adsorbing phosphate from wastewater in onsite wastewater treatment systems, *Front. Environ. Sci.* 8 (2020) 1–14, <https://doi.org/10.3389/fenvs.2020.538539>.
- [62] S.A.A.N. Almutkar, S.N. Abed, M. Scholz, Wetlands for wastewater treatment and subsequent recycling of treated effluent: a review, *Environ. Sci. Pollut. Res.* 25 (2018) 23595–23623, <https://doi.org/10.1007/s11356-018-2629-3>.

- [63] C. Tamulonis, Environmental Assessment of the Final Effluent Guidelines for Iron and Steel Industry, 2002. (<https://www.epa.gov/eg/iron-and-steel-manufacturing-effluent-guidelines-documents>).
- [64] E. Sugawara, H. Nikaido, Commission implementing decision (EU) 2018/1147 of 10 August 2018 establishing best available techniques (BAT) conclusions for waste treatment, under Directive 2010/75/EU of the European Parliament and of the Council, 2018. (<https://op.europa.eu/en/publication-detail/-/publication/a4de7e1b-a1e4-11e8-99ee-01aa75ed71a1/language-en>).
- [65] A.H. Kim, A.C. Yu, S.H. El Abbadi, K. Lu, D. Chan, E.A. Appel, C.S. Criddle, More than a fertilizer: wastewater-derived struvite as a high value, sustainable fire retardant, *Green Chem.* 23 (2021) 4510–4523, <https://doi.org/10.1039/d1gc00826a>.
- [66] J.P. Dhal, B.G. Mishra, G. Hota, Ferrous oxalate, maghemite and hematite nanorods as efficient adsorbents for decontamination of Congo red dye from aqueous system, *Int. J. Environ. Sci. Technol.* 12 (2015) 1845–1856, <https://doi.org/10.1007/s13762-014-0535-x>.
- [67] C. Li, Y. Ning, T. Yan, W. Zheng, Studies on nucleation and crystal growth kinetics of ferrous oxalate, *Heliyon* 5 (2019), e02758, <https://doi.org/10.1016/j.heliyon.2019.e02758>.
- [68] A. Whitaker, J.W. Jeffery, The crystal structure of struvite, $MgNH_4PO_4 \cdot 6H_2O$, *Acta Crystallogr. Sect. B Struct. Crystallogr. Cryst. Chem.* 26 (1970) 1429–1440, <https://doi.org/10.1107/s0567740870004284>.
- [69] M. Popko, I. Michalak, R. Wilk, M. Gramza, K. Chojnacka, H. Górecki, Effect of the new plant growth biostimulants based on amino acids on yield and grain quality of winter wheat, *Molecules* 23 (2018), <https://doi.org/10.3390/molecules23020470>.
- [70] K. Yetilmezsoy, E. Kocak, H.M. Akbin, D. Özçimen, Utilization of struvite recovered from high-strength ammonium-containing simulated wastewater as slow-release fertilizer and fire-retardant barrier, *Environ. Technol.* 41 (2020) 153–170, <https://doi.org/10.1080/09593330.2018.1491642>.